

RESEARCH ARTICLE

Anti-epileptic drug topiramate upregulates TGF β 1 and SOX9 expression in primary embryonic palatal mesenchyme cells: Implications for teratogenicity

Syed K. Rafi^{1*}, Jeremy P. Goering¹, Adam J. Olm-Shipman¹, Lauren A. Hipp¹, Nicholas J. Ernst¹, Nathan R. Wilson^{1#a}, Everett G. Hall^{1#b}, Sumedha Gunewardena², Irfan Saadi^{1*}

1 Department of Anatomy and Cell Biology, University of Kansas Medical Center, Kansas City, Kansas, United States of America, **2** Department of Molecular and Integrative Physiology, University of Kansas Medical Center, Kansas City, Kansas, United States of America

^{#a} Current address: Center for Regenerative Medicine, Massachusetts General Hospital, Harvard Medical School, Boston, Massachusetts, United States of America

^{#b} Current address: Clinical Research Training Center, Institute of Clinical and Translational Sciences, Washington University, St. Louis, Missouri, United States of America

* rafigene@yahoo.com (SKR); isaadi@kumc.edu (IS)



OPEN ACCESS

Citation: Rafi SK, Goering JP, Olm-Shipman AJ, Hipp LA, Ernst NJ, Wilson NR, et al. (2021) Anti-epileptic drug topiramate upregulates TGF β 1 and SOX9 expression in primary embryonic palatal mesenchyme cells: Implications for teratogenicity. *PLoS ONE* 16(2): e0246989. <https://doi.org/10.1371/journal.pone.0246989>

Editor: James A. Marrs, Indiana University-Purdue University Indianapolis, UNITED STATES

Received: September 1, 2020

Accepted: January 28, 2021

Published: February 12, 2021

Peer Review History: PLOS recognizes the benefits of transparency in the peer review process; therefore, we enable the publication of all of the content of peer review and author responses alongside final, published articles. The editorial history of this article is available here: <https://doi.org/10.1371/journal.pone.0246989>

Copyright: © 2021 Rafi et al. This is an open access article distributed under the terms of the [Creative Commons Attribution License](https://creativecommons.org/licenses/by/4.0/), which permits unrestricted use, distribution, and reproduction in any medium, provided the original author and source are credited.

Data Availability Statement: All relevant data are within the manuscript and its [Supporting Information](#) files.

Abstract

Topiramate is an anti-epileptic drug that is commonly prescribed not just to prevent seizures but also migraine headaches, with over 8 million prescriptions dispensed annually. Topiramate use during pregnancy has been linked to significantly increased risk of babies born with orofacial clefts (OFCs). However, the exact molecular mechanism of topiramate teratogenicity is unknown. In this study, we first used an unbiased antibody array analysis to test the effect of topiramate on human embryonic palatal mesenchyme (HEPM) cells. This analysis identified 40 differentially expressed proteins, showing strong connectivity to known genes associated with orofacial clefts. However, among known OFC genes, only TGF β 1 was significantly upregulated in the antibody array analysis. Next, we validated that topiramate could increase expression of TGF β 1 and of downstream target phospho-SMAD2 in primary mouse embryonic palatal mesenchyme (MEPM) cells. Furthermore, we showed that topiramate treatment of primary MEPM cells increased expression of SOX9. SOX9 overexpression in chondrocytes is known to cause cleft palate in mouse. We propose that topiramate mediates upregulation of TGF β 1 signaling through activation of γ -aminobutyric acid (GABA) receptors in the palate. TGF β 1 and SOX9 play critical roles in orofacial morphogenesis, and their abnormal overexpression provides a plausible etiologic molecular mechanism for the teratogenic effects of topiramate.

Introduction

Topiramate is an anti-epileptic drug that was approved by the U.S. Food and Drug Administration (FDA) for the treatment of partial onset or primary generalized tonic-clonic seizures in

Funding: This project was supported in part by the National Institutes of Health Center of Biomedical Research Excellence (COBRE) grant (National Institute of General Medical Sciences P20 GM104936 and P30 GM122731, I.S.), Kansas IDeA Network for Biomedical Research Excellence grant (National Institute of General Medical Sciences P20 GM103418, I.S.), Kansas Intellectual and Developmental Disabilities Research Center grant (U54 Eunice Kennedy Shriver National Institute of Child Health and Human Development, HD090216, I.S. and S.G.), and a National Institute of Dental and Craniofacial Research grant (DE026172, I.S.).

Competing interests: The authors do not have any competing financial interests pertaining to the studies presented here.

1996 and for migraine prophylaxis in 2004. Topiramate is currently used either as a monotherapy or an adjunctive therapy to treat migraines, partial-onset seizures, primary generalized tonic-clonic seizures, and other seizure disorders. In addition, topiramate has been used off-label for binge-eating disorder [1], bulimia nervosa [2], alcohol use disorder [3], anti-psychotic induced weight gain [4], and essential tremor [5]. Verispan's Vector One®: National (VONA) and IQVIA's Total Patient Tracker® (TPT) reported that, between January 2007 and December 2010, approximately 4.3 million patients filled 32.3 million topiramate prescriptions (FDA Drug Safety Communication, 03-04-2011). This number has risen to approximately 4.1 million patients receiving a prescription for topiramate between March 2014 and February 2016 (FDA Pediatric Post-marketing Pharmacovigilance and Drug Utilization Review for topiramate; June 20, 2016). According to estimates in the United States alone, approximately 1.3 million epileptic women are of childbearing age [6], and approximately 24,000 children are born annually to epileptic mothers (North American Antiepileptic Drug Pregnancy Registry) [7]. Thus, control of seizures during pregnancy is an important public health challenge, as women with epilepsy have a higher risk of peripartum complications including stillbirth, preeclampsia, preterm labor, and a 10-fold increase in mortality compared to women without epilepsy [8]. Importantly, in a recent study [9], twice as many women with migraines (46%) were prescribed topiramate than women with epilepsy or seizures (20%), exposing an even larger proportion of women of childbearing age to potential topiramate teratogenicity.

Topiramate use during pregnancy has been linked to a significantly increased risk of birth defects affecting orofacial, cardiac and urogenital development [10–12]. Multiple studies have reported that the incidence of oral clefts in particular is increased in topiramate-exposed pregnancies [10, 11, 13, 14]. In the North American Antiepileptic Drug Pregnancy Registry [15], the relative risk of oral clefts in topiramate-exposed pregnancies was ~13-fold higher than the general risk in births [16]. The FDA has now changed the classification of topiramate from a pregnancy-C category to a pregnancy-D category drug, warning that topiramate can cause fetal harm when administered to a pregnant woman (FDA Drug Safety Communication, 03-04-2011). Despite broad use and teratogenic potential of topiramate, the molecular mechanism(s) underlying the increased occurrence of major congenital malformations is not understood [6, 7, 11, 13, 17].

We sought to identify molecular clues to the teratogenic effect of topiramate on palate development. Normal palate development during embryogenesis is a multistep process that begins with bilateral vertical growth of the palatal shelves adjacent to the tongue till embryonic day 13.5 (E13.5). These shelves then elevate above the tongue, move horizontally and fuse in the midline to form the palate by E15.5. The palatal shelf is mainly composed of the oral ectoderm derived epithelial cells and the neural crest derived mesenchymal cells. Defects in neural crest function are sufficient to cause cleft palate [18, 19]. To investigate the potential effect of topiramate exposure on palate development, we first treated human embryonic palate mesenchyme (HEPM) cells with a high dose of topiramate, then performed an unbiased exploratory antibody-array approach to identify misregulated proteins. Our analysis showed upregulation of transforming growth factor beta one (TGF β 1) expression and altered activation of cell survival networks. We then validated our findings in primary mouse embryonic palate mesenchyme (MEPM) cells following exposure to a range of topiramate concentrations. We showed that TGF β 1 levels are indeed upregulated even at physiological 50 μ M topiramate treatment for six hours. Topiramate treatment of primary MEPM cells also increased expression of SRY-Box Transcription Factor 9 (SOX9), a TGF β 1 target that causes cleft palate when abnormally expressed. We propose that perturbation of TGF β pathway and SOX9 expression through γ -aminobutyric acid (GABA) receptors in the embryonic palate represents a plausible etiologic mechanism underlying topiramate-induced oral clefts.

Materials and methods

Culture of HEPM cell line

Human embryonic palatal mesenchyme (HEPM) cells, available commercially (ATCC, CRL-1486), were cultured in DMEM media, with high concentration of glucose and pyruvate, supplemented with 10% fetal bovine serum and penicillin/streptomycin. The HEPM cells were kept at low passage numbers and inspected visually for signs of differentiation. Topiramate (Sigma-Aldrich, St. Louis, MO) was resuspended in ethanol. HEPM cells were treated with 1000 μ M topiramate and cultured at 37°C for 6 hours. Cells were briefly washed with PBS, scraped and flash-frozen for subsequent RNA and protein extraction.

Isolation and culture of primary MEPM cells

Palatal shelves were excised from wildtype E13.5 mouse embryos. Briefly, the embryo heads were cut, followed by removal of the lower jaw and tongue, thus exposing the palatal shelves. The palatal shelves were subsequently dissected, and the cells dissociated into a single-cell suspension by incubating the palatal shelves in 0.25% Trypsin for 10 minutes and then vigorously pipetting up and down to mechanically separate the cells. The resulting Mouse Embryonic Palatal Mesenchyme (MEPM) cells were then cultured in Dulbecco's Modified Eagle Medium (DMEM) with high glucose and supplemented with 10% Fetal Bovine Serum and Penicillin/Streptomycin. MEPMs were used fresh, never-passaged, before drug treatment. MEPM cells were treated with 25, 50 or 100 μ M topiramate (APEXBio, Houston, TX) and incubated for 6 hours at 37°C. GABA inhibitor (10 μ M), flumazenil (APEXBio, Houston, TX), was added with 50 μ M topiramate for the 6 hour treatment duration. Ethanol was used for vehicle treatment. All experiments involving animals were carried out with a protocol approved by the University of Kansas Medical Center (KUMC) Institutional Animal Care and Use Committee, in accordance with their guidelines and regulations (Protocol Number: 2018–2447). The experiments reported in this study are from 12 timed-pregnant C57BL/6J female mice (The Jackson Laboratory, Bar Harbor, ME) that were euthanized using a CO₂ chamber followed by harvesting of E13.5 embryos.

Antibody array analysis

Protein extracts from HEPM cells with vehicle (Control) or with topiramate treatment (1000 μ M for 6 hours) were analyzed by Full Moon BioSystems (Sunnyvale, CA) Cell Signaling Explorer antibody arrays (SET100), according to manufacturer's protocol. Briefly, control and topiramate-treated HEPM cell lysates were labeled with Cy3 fluorophore using the antibody array assay kit from Full Moon BioSystems (KAS02). Antibody array slides were independently incubated with labeled lysates, washed, and scanned using microarray scanner from Agilent (Santa Clara, CA).

Statistical analysis of antibody array data

Each antibody array comprised of two technical replicates. The experiment was performed in biological duplicates for downstream statistical analysis. Each probe from each of the biological and technical replicates was first determined to be significantly expressed relative to its background intensity. This significance calculation was based on a ≤ 0.05 cutoff of the Benjamini and Hochberg [20] adjusted p-value of the t-statistic of the difference between the mean expression (F532 mean) and mean background (B532 mean) intensities. A gene was regarded as not significantly expressed under a particular treatment if any one of its biological replicates was not significantly expressed. The first filtering step removed all genes that were not

significantly expressed in either one of the treatment groups. The remaining probes were background corrected using a modified Robust Multi-array Average (RMA) [21] algorithm for protein arrays. The background adjusted probes were log transformed (base 2) and quantile normalized. Technical replicates were then averaged (geometric average) to give the background adjusted normalized expression for each biological replicate. A two-way ANOVA model (factor 1: treatment with levels Control and topiramate treated; factor 2: antibody array with levels array 1 and array 2) was fitted to the data to determine the gene level significance of the difference in expression between Control and topiramate treated samples. Protein expression with a p-value ≤ 0.05 and absolute fold change ≥ 1.15 were deemed sufficiently differentially expressed for protein arrays, yielding 40 proteins for further analysis.

Gene interaction analysis

The Ingenuity Pathway Analysis software (IPA, Qiagen, www.qiagenbioinformatics.com) was used to build a gene interaction network of the 40 differentially expressed proteins and 107 known genes associated with orofacial clefts identified by IPA. The aim was to establish a single network of interactions between as many of the 40 differentially expressed proteins from the antibody array and the 107 genes associated with orofacial clefts. IPA performs this task with the aid of its knowledge database consisting of literature-based curated information on genes and gene product interactions.

Quantitative PCR analysis

Quantitative PCR (qPCR) analysis was used to test expression of the *TGFB1* in HEPM cells treated with 1mM Topiramate for 6 hours and *Tgfb1* in MEPM cells treated with 50 μ M Topiramate for 6 hours. RNA was extracted using NucleoSpin RNA XS kit (Takara, Kusatsu, Japan). 1 μ g of RNA from each sample was used to generate cDNA with qScript cDNA SuperMix (QuantaBio, Beverly, MA). *OAZ1* and *B2m* housekeeping genes were used to normalize data for HEPM and MEPM cells, respectively. Analysis was performed on 4–5 sets of biological replicates, each with 2 technical replicates per gene. Statistical significance was calculated using a Student's t-test. Primer sequences are listed in S1 Fig.

Western blotting

For protein extraction, MEPM cells were briefly washed with PBS, scraped and either flash-frozen or lysed immediately. Cells were lysed by suspension in radioimmunoprecipitation assay (RIPA) buffer with HALT protease inhibitor Cocktail (Thermo Scientific, Waltham, MA) and by agitation for 30 minutes at 4°C. Cell lysates were centrifuged for 10 minutes at 13,000 rcf and the protein extracts (supernatant) collected. Lysates were then electrophoresed in 4–15% gradient Mini-Protean TGX Stain-Free precast gels (Bio-RAD, Hercules, CA). After electrophoresis, the gels were exposed to UV light for 45 seconds to develop the total protein signal and imaged on a ChemiDoc System (Bio-RAD, Hercules, CA) before being transferred onto Immobilon PVDF membranes (EMD Millipore, Billerica, MA). PVDF membranes were then blocked in Odyssey Blocking Buffer (Li-Cor, Lincoln, NE) either overnight at 4°C or at room temperature for 1 hour. Primary antibodies used were anti-TGF β 1 (1:1000; Abcepta, AP12348A, Cambridge, MA), anti-phospho-SMAD2 (1:5000; Cell Signaling Technologies, 3108, Danvers, MA), anti-SMAD2 (1:5000; Cell Signaling Technologies, 5339, Danvers, MA) and anti-SOX9 (1:5000; Abcepta, AM1964b, San Diego, CA), and anti-SOX10 (1:5000; Aviva Systems, ARP33326, San Diego, CA). Secondary antibodies used were HRP-linked goat anti-rabbit IgG (1:10,000; Cell Signaling Technologies, Danvers, MA) and HRP-linked goat anti-mouse IgG (1:10,000; Santa Cruz Biotechnologies, Dallas, TX). Femto SuperSignal West ECL

reagent (Thermo Scientific, Waltham, MA) was used to develop the signal. Image Lab software (Bio Rad, Hercules, CA) was used to quantitate total protein and western blot intensity. Each blot was normalized to the total protein loaded, and then fold change calculated by dividing total drug-treated samples by vehicle-treated sample.

Immunofluorescence and imaging analysis

MEPM cells, cultured as described above, were fixed in 4% paraformaldehyde (PFA) for 10 min, blocked in phosphate buffered saline (PBS) with 1% goat serum and 0.1% Tween, and stained using Anti-TGFβ1 (1:1000; Abcam, Cambridge, MA). After staining, coverslips were mounted in containing DAPI (Vector Labs, Burlingame, CA). Individual cells were imaged, and the levels of TGFβ1 fluorescence were quantitated in at least 30 cells per treatment from 3 independent experiments using NIH ImageJ software. Briefly, we used NIH ImageJ to calculate the corrected total cell fluorescence (CTCF) in each cell, using the formula: $CTCF = \text{Integrated Density} - (\text{Area of selected cell} \times \text{Mean fluorescence of background readings})$.

Results

Antibody-array-based analysis of HEPM cells following topiramate treatment

Protein extracts from HEPM cells with supra-physiological topiramate treatment (1000 μM for 6 hours) or without the treatment (Control) were assayed by Full Moon BioSystems (Sunnyvale, CA) Cell Signaling Explorer antibody-array. The Cell Signaling Explorer array includes antibodies for 1358 individual proteins, in two technical replicates, encompassing 20 cellular pathways. The antibody array experiment was performed with two biological replicates. The results were analyzed for statistical significance as described in the Materials and Methods section. Protein levels of 57 gene products were significantly altered ($p < 0.05$, [S1 Table](#)). We used a 1.15-fold cutoff ($|FC| \geq 1.15$) [22, 23], resulting in 40 differentially expressed proteins with 19 proteins downregulated and 21 upregulated ([Table 1](#)). To determine the importance of these 40 altered gene products to orofacial morphogenesis and OFCs, we used Ingenuity Systems pathway analysis (IPA) as well as manual literature curation.

IPA analysis of proteins with altered expression following topiramate treatment shows connectivity with genes associated with orofacial clefts

The antibody array analysis identified statistically significant changes in expression of 40 proteins following topiramate treatment ([Table 1](#); $p < 0.05$, $|FC| \geq 1.15$). Separately, IPA software reported 107 known genes associated with orofacial clefts ([S2 Table](#)). Only 18 of the 107 OFC genes were represented on the Full Moon BioSystems Cell Signaling Explorer antibody array. Among these 18 proteins encoded by OFC genes, only TGFβ1 was significantly altered (increased) upon topiramate treatment of HEPM cells.

We also analyzed the 40 gene products with IPA for changes in diseases and bio-functions ([S3 Table](#)). The top predicted categories were related to “cell death and survival”, and “organismal growth and development”. Overall, IPA predicted that topiramate treatment decreased cell viability ([S3 Table](#); IPA Ranks 13, 29) and increased apoptosis ([S3 Table](#); IPA Rank 37). However, IPA also correctly predicted increased cell viability of neurons ([S3 Table](#); IPA Rank 7) [24], consistent with a cell-type specific effect of topiramate. The top IPA predicted networks also indicated an effect on cell growth and survival pathways ([S4 Table](#)). Next, we looked at connectivity of the genes encoding the 40 altered proteins to the IPA-reported 107 genes

Table 1. List of 40 proteins with statistically significant change in expression and a 1.15-fold-change cut-off in HEPM cells following topiramate treatment.

<i>Protein Name</i>	<i>Symbol</i>	<i>UniProtKB ID</i>	<i>Antibody Array ID</i>	<i>Fold Change</i>
Checkpoint kinase 2	CHEK2	O96017	659	1.96
Low-density lipoprotein receptor class A domain-containing protein 1	LDLRAD1 / LRP1	Q5T700	109	1.64
Aldehyde dehydrogenase 7	ALDH3B1	P43353	92	1.46
NADPH oxidase 5	NOX5	Q96PH1	282	1.46
Proto-oncogene tyrosine-protein kinase receptor Ret	RET	P07949	490	1.42
Cardiac troponin I	TNNI3(cTnl)	P19429	146	1.39
Transforming Growth Factor beta 1	TGFB1	P01137	377	1.39
Unconventional myosin Id	MYO1D	O94832	276	1.37
Tyrosine-protein kinase receptor 3	TYRO3	Q06418	478	1.33
Cyclosome 1	APC1	Q9H1A4	1093	1.32
Superoxide dismutase 1	SOD1	P00441	996	1.31
Oral cancer-overexpressed protein 1	ORAV1 / ORAOV1	Q8WV07	1078	1.30
Growth arrest and DNA damage-inducible proteins-interacting protein 1	GADD45GIP1	Q8TAE8	1285	1.27
Phosphatidylinositol-glycan biosynthesis class H protein	PIGH	Q14442	453	1.25
CD30 Ligand	CD153	P32971	220	1.24
Patched	PTCH1	Q13635	35	1.23
Cadherin-10, T2-cadherin	CDH10	Q9Y6N8	415	1.21
ATP synthase subunit delta, mitochondrial	ATP5D	P30049	261	1.19
TNF Receptor1-associated DEATH domain protein	TRADD /TNFR1	Q15628	716	1.19
Alcohol dehydrogenase class 4 mu/sigma chain	ADH7	P40394	91	1.19
Interferon Regulatory Factor 4	IRF4	Q15306	730	1.18
Bcl10-interacting CARD protein	C9ORF89	Q96LW7	422	-1.15
S-phase kinase-associated protein 1	SKP1A/p19	P63208	363	-1.16
B melanoma antigen 3/ Cancer/testis antigen 2.3	BAGE3	Q86Y29	420	-1.20
Cancer-associated Gene Protein	ATBP3 / MTUS1	Q7Z7A3	907	-1.20
SUMO1-activating enzyme 2	UBA2	Q9UBT2	874	-1.22
Tissue inhibitor of metalloproteinases 2	TIMP2	P16035	537	-1.22
RING finger and WD repeat domain protein 2	RFWD2	Q8NHY2	1107	-1.23
Coagulation factor VII (light chain, Cleaved-Arg212)	FA7	P08709	1156	-1.29
Rho guanine nucleotide exchange factor 3	ARHGEF3	Q9NR81	1123	-1.30
Cytochrome c oxidase assembly protein COX11	COX11	Q9Y6N1	911	-1.31
Diacylglycerol Kinase eta	DGKH	Q86XP1	908	-1.36
ATP-binding cassette sub-family A member 8	ABCA8	O94911	848	-1.37
Shugoshin-like 1	SGOL1	Q5FBB7	895	-1.37
Guanylate Cyclase Beta 1	GUCY1B3	Q02153	853	-1.38
Cell division cycle 7 related kinase	CDC7	O00311	1044	-1.38
Aldo-keto reductase family 1 member C-like protein 1	AKR1CL1	Q5T2L2	246	-1.41
Interleukin 2	IL2	P60568	832	-1.55
Cytochrome P450 7B1	CYP7B1	O75881	802	-1.82
Ubiquitin-protein ligase E3B	UBE3B	Q7Z3V4	291	-2.19

<https://doi.org/10.1371/journal.pone.0246989.t001>

associated with orofacial clefts (Fig 1). TGFβ1 was the only OFC gene among the 40 topiramate-altered proteins in our analysis. A single network was able to connect 22 (9 downregulated, 13 upregulated) of these 40 (55%) genes encoding differentially expressed proteins to 87 OFC genes (81%), either directly or indirectly. TGFβ1 showed the highest number of connections to known genes associated with orofacial clefts (Fig 1). Therefore, we focused our validation studies on TGFβ1.

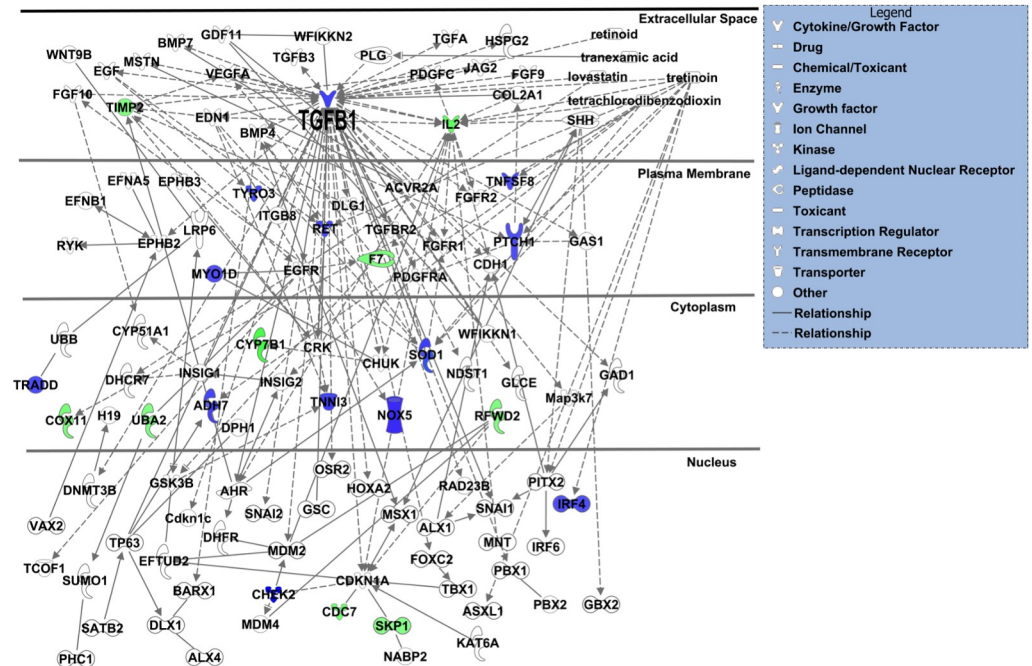


Fig 1. TGFβ1 showed highest connectivity in IPA-generated network of differentially expressed gene products from topiramate-treated HEPM cells and known orofacial clefting-associated genes. The 40 gene products with differential expression following 6-hour, 1000μM topiramate treatment of HEPM cells were analyzed with Ingenuity Systems pathway analysis (IPA) software for possible interaction with 107 IPA-identified genes associated with orofacial clefts. A single resulting network accounted for 22 (55%) of the topiramate-treated HEPM genes in association with 87 (81%) known OFC-related genes. The upregulated or downregulated genes from the HEPM data were colored blue or green, respectively. The only gene common between the two datasets was *TGFβ1*, which also displays the highest connectivity in the network.

<https://doi.org/10.1371/journal.pone.0246989.g001>

Validation of TGFβ1 upregulation in primary Mouse Embryonic Palate Mesenchyme (MEPM) cells following treatment with physiological levels of topiramate

Our analysis indicated TGFβ1 as the central molecule affected by topiramate treatment of HEPM cells. To confirm that our finding was not an artifact of using an immortalized cell line and supraphysiological levels of topiramate, we used primary MEPM cells and physiological topiramate doses. The peak serum level for even topiramate monotherapy is approximately 25–50 μM [25–27]. Therefore, we initially included both the physiological 50 μM concentration and two supraphysiological concentrations to treat fresh primary MEPM cells from E13.5 embryonic palates for 6 hours (Fig 2A–2E). Following treatment, cells were fixed and immunostained using an anti-TGFβ1 antibody (Fig 2A–2D). Individual cells were imaged, and the levels of TGFβ1 were quantitated using NIH ImageJ software. The experiment was repeated three times with different primary MEPM isolations. We saw a significant increase in intracellular TGFβ1 level at the physiological 50μM topiramate treatment (Fig 2E).

We also performed Western blot analysis following 25μM and 50μM topiramate treatments (Fig 2F) and showed a significant increase with 50μM topiramate (Fig 2G). There was no increase in *TGFβ1* (HEPM) or *Tgfb1* (MEPM) mRNA transcripts at the end of the 6-hour topiramate treatment (S1 Fig). To test for an upregulation of the TGFβ1 signaling pathway, we also assessed levels of phospho-SMAD2 (P-SMAD2), a downstream effector molecule (transcription factor) of the ligand-bound TGFβ receptor that requires phosphorylation to

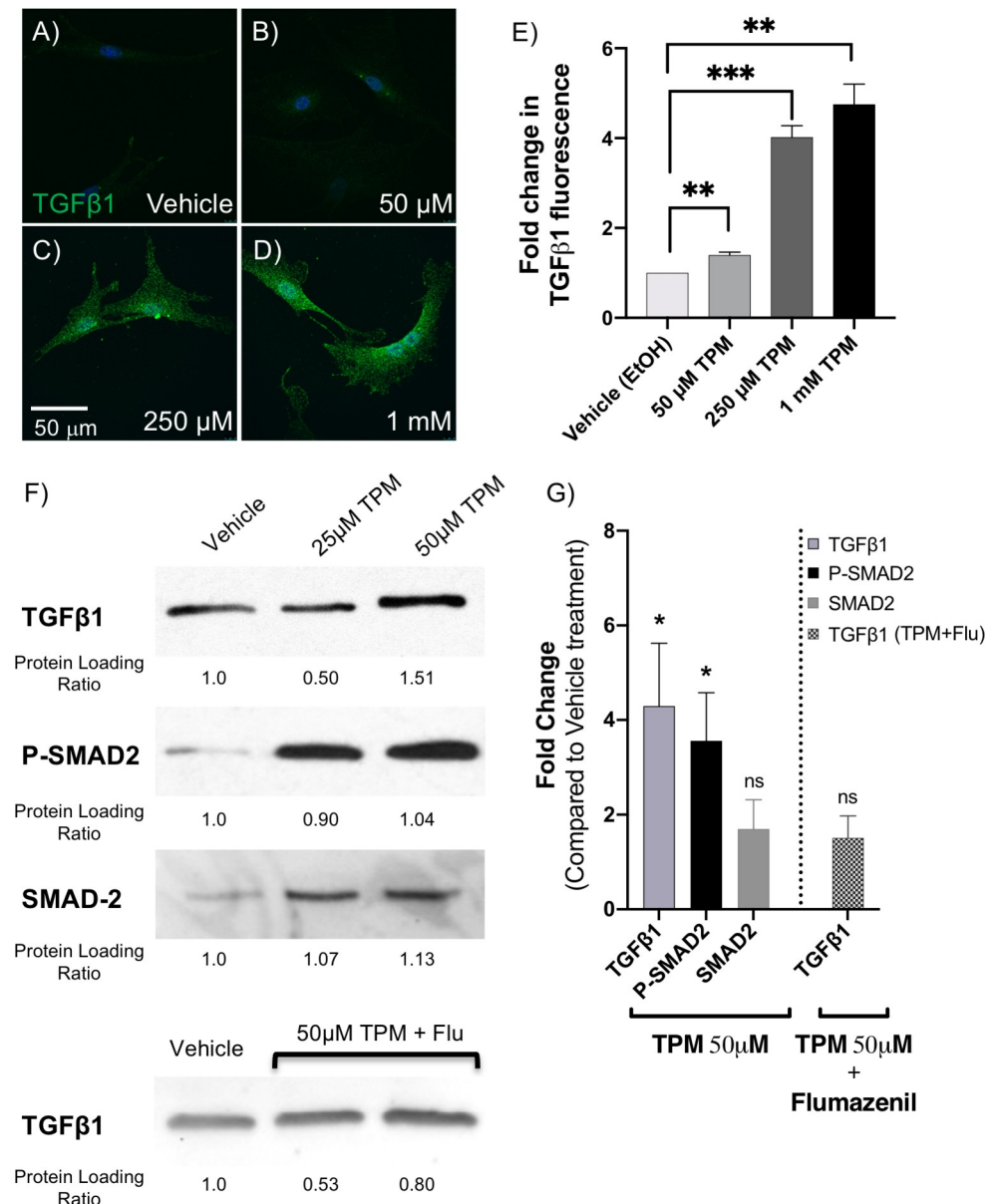


Fig 2. Topiramate treatment of primary MEPM cells upregulated TGFβ1 expression via GABA receptors. To validate upregulation of TGFβ1, we isolated primary mouse embryonic palate mesenchyme (MEPM) cells from E13.5 embryos and treated them with 25 μM, 50 μM, 250 μM or 1 mM topiramate for 6 hours, as indicated. These cells were analyzed for TGFβ1 expression by immunostaining (A-E) and Western blotting (F-G). There was a significant increase in intracellular TGFβ1 expression upon as little as 50 μM topiramate treatment (A-E), which was quantitated in at least 30 cells per treatment from 3 independent experiments (**, $p < 0.003$; ***, $p < 0.0003$). The scale bar represents 50 μm (A-D). Western blot analysis also showed a significant increase upon treatment with 50 μM topiramate (F, G). We also showed increased phospho-SMAD2 (P-SMAD2) levels with both 25 μM and 50 μM topiramate treatments (F, G), indicating an upregulation of TGFβ1 signaling cascade (*, $p < 0.019$). No significant changes were observed in total SMAD-2 level upon 50 μM topiramate treatment (F, G). The upregulation of TGFβ1 protein expression upon 50 μM topiramate treatment is blunted in the presence of 10 μM GABA receptor inhibitor, Flumazenil (F, G).

<https://doi.org/10.1371/journal.pone.0246989.g002>

translocate to the nucleus. Indeed, P-SMAD2 levels were increased following both 25 μM and 50 μM topiramate treatment (Fig 2F and 2G), indicating a strong upregulation of TGFβ signaling via SMAD-dependent pathway.

Topiramate treatment increased TGF β 1 protein level via GABA receptors

Since topiramate has been reported to upregulate GABA levels and GABA_A receptor-based signaling [28], which in turn has been shown in other systems to increase TGF β levels [29, 30], we wanted to see if the same was true in MEPM cells. Thus, we treated the MEPM cells with 50 μ M topiramate in the presence of 10 μ M flumazenil, a selective inhibitor of GABA_A receptors [31]. Indeed, flumazenil was able to blunt the effect of topiramate on TGF β 1 level (Fig 2F and 2G), indicating that topiramate was mediating its effect through GABA_A receptors.

Topiramate treatment of primary MEPM cells results in increased SOX9 expression

After validating the involvement of TGF β signaling, we wanted to look at a TGF β target gene with a role in orofacial clefting. We decided to look at expression of SOX9, a transcription factor belonging to the SOXE group with a key role in regulating chondrocyte function [32, 33]. SOX9 mutations have been identified in patients with Pierre Robin sequence [34] and campomelic (or acampomelic) dysplasia with or without sex reversal [35, 36]. Pierre Robin sequence is a series of defects including small jaw, a posteriorly placed tongue and cleft palate [34]. Campomelic dysplasia is an autosomal dominant skeletal disorder that is characterized by bowed limbs, hypoplastic or hypomineralized bones, and small chest size. Cleft palate, micrognathia (including Pierre Robin sequence), flat face and hypertelorism are also frequent features of Campomelic dysplasia. Interestingly, SOX9 mutations in patients with Pierre Robin sequence were located in the regulatory region affecting SOX9 expression. Furthermore, both knock-down and overexpression of *Sox9* in mouse has been shown to result in cleft palate phenotypes [32, 33, 37]. Therefore, an effect on SOX9 expression downstream of TGF β 1 in our system would represent a plausible pathogenetic mechanism of topiramate-based facial clefts. Indeed, we found that SOX9 expression is increased following topiramate treatment (Fig 3A and 3B), which is consistent with a role for TGF β 1 in stabilizing SOX9 protein [38]. Expression of another SOXE transcription factor group member associated with orofacial clefts, SOX10, is not altered upon topiramate treatment (Fig 3A and 3C), showing specificity for SOX9

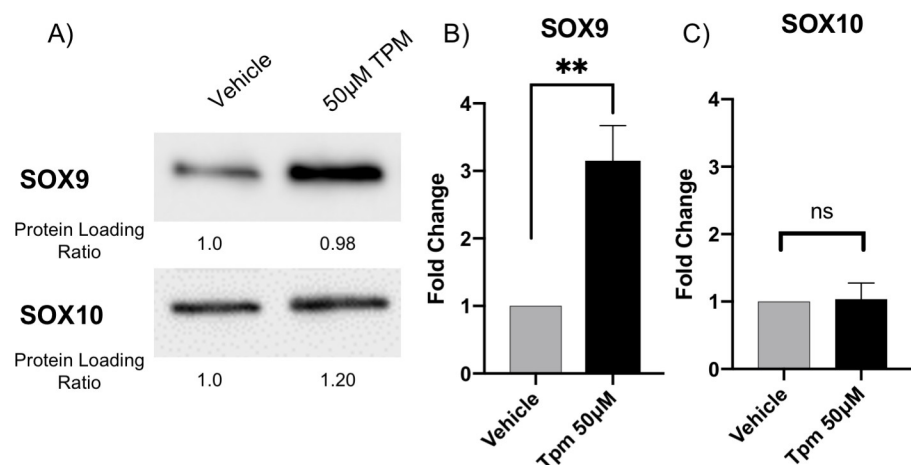


Fig 3. Topiramate treatment of primary MEPM cells resulted in increased SOX9 expression. We looked at expression of SOX9, a TGF β 1 target gene involved in orofacial clefting. Western blot analysis of topiramate-treated primary MEPM cells resulted in statistically significant increase in SOX9 expression (A,B; **, $p < 0.006$). In contrast, expression of SOX10 is not altered upon topiramate treatment (A,C; ns, not significant).

<https://doi.org/10.1371/journal.pone.0246989.g003>

upregulation. Our results with topiramate suggest that TGF β 1-mediated altered expression of SOX9 underlies the teratogenicity of this antiepileptic drug.

Discussion

We utilized an unbiased cell signaling antibody array to identify 40 proteins with altered expression following topiramate treatment of HEPM cells. Although a smaller number of proteins were analyzed with the antibody array compared to an RNA-based analysis, our data suggest that the protein-based analysis provided a clearer view of signaling changes. These 40 proteins included TGF β 1, which was significantly upregulated and was the only one associated with cleft palate.

During palatogenesis, all three TGF β ligands—TGF β 1, TGF β 2 and TGF β 3—are expressed in the palatal shelves. TGF β 1 is strongly expressed in the distal pre-fusion palatal shelves [39]. Therefore, we utilized primary MEPM cells to validate TGF β 1 increase upon topiramate treatment. In humans, increase in TGF β signaling has been identified in Marfan and Loeys-Dietz syndromes [40–42]. Marfan syndrome patients show overgrowth of the long bones of the arms and legs, and have defects in multiple organ systems including cardiovascular, craniofacial and ocular anomalies. Individuals with Loeys-Dietz syndrome also have cardiovascular and skeletal abnormalities that are more severe than in Marfan syndrome. Craniofacial defects in Loeys-Dietz syndrome patients include craniosynostosis and cleft palate. TGF β 1 has been shown to be a potent inducer of growth inhibition in various cell types [43–45]. However, in palate development, some evidence suggests TGF β ligands can promote cell proliferation [46]. Regardless of the complex function of individual TGF β pathway molecules, perturbation of TGF β signaling affects many genes associated with orofacial clefts [46, 47] that can negatively impact palatogenesis.

To show that TGF β 1 increase can affect downstream genes associated with orofacial clefts, we looked at expression of SOX9 transcription factor. Deficiency of SOX9 leads to Campomelic dysplasia, characterized by facial and skeletal anomalies, including cleft palate, midface hypoplasia, short stature and short and bowed limbs [35, 36]. However, we actually observed an increase in SOX9 levels following topiramate treatment. TGF β -mediated increase in SOX9 expression has also been recently shown in mesenchymal fibroblasts to promote renal fibrosis [48]. Importantly, when SOX9 is overexpressed in all chondrocytes, by insertion of *Sox9* cDNA into the *Col2a1* locus, it also results in cleft palate phenotype [32]. Thus, perturbation of SOX9 expression in either direction affects palatogenesis. A sudden surge in TGF β 1 level would therefore disrupt this delicate regulation of SOX9 expression in the palate mesenchyme, and thus result in OFC.

Phosphorylation of SMAD2, a downstream effector of the TGF β pathway, is necessary for the stabilization of *Sox9* in palatogenesis [38]. Phospho-SMAD2 was upregulated in topiramate-treated MEPM cells, validating that topiramate increases TGF β signaling cascade. In a recent study examining the effects of topical topiramate on wound healing using mice found significantly increased levels of TGF β and SOX2 in epidermal cells treated with topiramate [49], which is consistent with a topiramate-TGF β -SOX cascade observed in our analysis.

Antiepileptic drugs ameliorate CNS excitatory seizures by dampening overall neuronal activity. This includes downregulation of excitatory signals from glutamate receptors and upregulation of inhibitory signals from GABA receptors [50]. Topiramate has been reported to upregulate GABA levels and GABA_A receptor-based signaling [28]. Importantly, increased GABA signaling upregulates TGF β levels [29, 30]. While mouse mutants for some components of the GABA signaling pathway result in cleft palate phenotype [51–53], the effect of GABA upregulation on palatogenesis has not been explored. Recently, upregulation of GABA

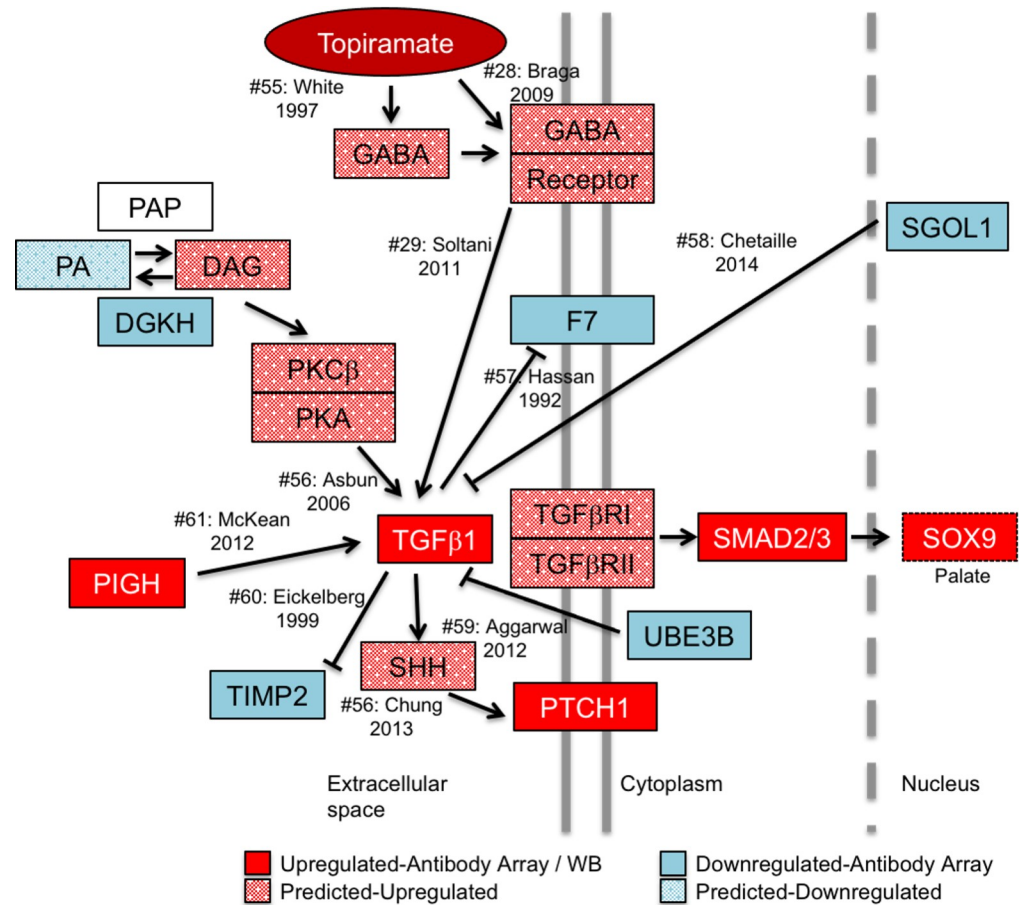


Fig 4. Model of topiramate action on MEPM cells. Our model predicts that topiramate is capable of stimulating GABA receptors in the palate to upregulate TGFβ1 expression. TGFβ1 expression is tightly regulated during craniofacial morphogenesis. Dysregulation of TGFβ1 signaling can lead to altered expression of genes associated with orofacial clefts. For example, we show that topiramate leads to upregulation of SOX9 expression, which is sufficient to result in cleft palate in mice. In order to gather corroborating evidence for the upregulation of TGFβ signaling from the 39 (excluding TGFβ) differentially expressed gene products, we performed a manual curation of the literature for connectivity to TGFβ1. Our analysis revealed that changes in an additional seven (18%) of the proteins are consistent with upregulation of TGFβ1 signaling. Moreover, these molecules affect TGFβ1 signaling both upstream and downstream of the TGFβ1 ligand, suggesting a concerted global upregulation of the pathway. The solid-colored molecules are from the antibody-array or western blot results, while the spotted molecules are changes in upstream effectors predicted from literature. Citation number (#) corresponds to listed references.

<https://doi.org/10.1371/journal.pone.0246989.g004>

receptor activity was shown to decrease cell proliferation of embryonic and neural crest cells, as well as of blastocysts [54]. These results are consistent with a potential inhibitory effect of GABA upregulation on overall embryonic development and, in particular, on neural crest-influenced orofacial morphogenesis [18]. Also in support, several studies indicate tissue-specific activation of cell death following upregulation of TGFβ signaling, as reviewed in Schuster and Kriegelstein [45]. Thus, our data suggest that topiramate-based upregulation of GABA signaling can increase TGFβ signaling, which in turn results in tissue-specific changes in expression of downstream genes, such as SOX9, involved in palatogenesis.

To assess the impact of the genes encoding the 40 differentially expressed proteins on orofacial clefting, we assayed their connectivity to the 107 known OFC-related genes reported by IPA. A single IPA connectivity network included over 55% of both sets of genes (Fig 1). This high level of connectivity argues that exposure to topiramate has the potential to perturb many

OFC-related genes and pathways in the developing palate. The highest connectivity in this network was centered on TGFβ1 ligand. We also considered the possibility that the upregulation extended beyond TGFβ1 ligand to the entire pathway. We reasoned that if TGFβ signaling was indeed upregulated in topiramate-treated HEPM cells, we would find evidence for upregulation of downstream factors from our antibody array data. Indeed, a manually curated network showed evidence for upregulation of TGFβ signaling both upstream and downstream of TGFβ1 ligand (Fig 4) [28, 29, 55–62]. We were able to directly confirm nine molecules that were consistent with upregulation of TGFβ signaling (Fig 4: PIGH, PTCH1, SMAD2/3, SOX9, DGKH, F7, SGOL1, TIMP2, UBE3B). We also found literature support for the topiramate-based increase in GABA signaling [28, 55] to in turn upregulate levels of TGFβ1 [29], which is consistent with our result showing flumazenil blunts this effect. Together, this network not only shows a broad upregulation of the TGFβ signaling pathway following topiramate treatment of HEPM cells, but also suggests perturbation of other signaling pathways important in embryogenesis, including Phospholipase-C-based PKC/PKA and Sonic hedgehog signaling (Fig 4).

The genetic network affected by topiramate treatment of palate mesenchyme cells provides an important framework to study the OFC-related teratogenic effects. Future *in vitro* and *in vivo* studies are required to elucidate the precise role of increased TGFβ signaling in the teratogenicity of topiramate. Topiramate is one of many anti-epileptic and mood-stabilizing drugs that have recently been associated with structural birth defects. All of these drugs share certain molecular characteristics and targets. Therefore, understanding the molecular genetic mechanism behind topiramate teratogenicity will likely also provide clues to the general link reported among a broad class of antiepileptic drugs and birth defects.

Supporting information

S1 Fig. Topiramate treatment of HEPM and MEPM cells did not increase TGFB1 transcript level. A) RNA from HEPM cells treated for 6 hours with vehicle (control) and 1mM Topiramate (Tpm) was analyzed for *TGFB1* expression using qRT-PCR. No increase was observed upon treatment. Data show average and SEM from 4 pairs of treatments. B) RNA from MEPM cells treated for 6 hours with vehicle and 50uM Tpm was analyzed for *Tgfb1* expression using qRT-PCR. Data are shown from 5 experiments. No significant change was observed between vehicle and treatment. ns = not significant.

(TIF)

S1 Table. List of all 57 proteins with altered expression in topiramate-treated HEPM cells.

(TIF)

S2 Table. List of IPA predicted OFC-related genes.

(TIF)

S3 Table. IPA predicted diseases and bio-functions associated with the 40 gene-products significantly altered in topiramate-treated HEPM cells.

(TIF)

S4 Table. IPA predicted networks associated with the 40 gene-products significantly altered in topiramate-treated HEPM cells.

(TIF)

S1 Raw images.

(PDF)

Acknowledgments

We thank Dr. Partha Kasturi and Dr. Hemantkumar Chavan (KUMC) for assistance and use of their equipment; Dr. Karin Zueckert-Gaudenz and Mr. Brian Flaherty (Molecular Biology Core, Stowers Institute for Medical Research, Kansas City, MO) for use of their microarray scanners; Ms. Shannon Zhang (Full Moon BioSystems Inc.) for assistance with antibody array data analysis; Mr. Byunggil Yoo (KUMC) for assistance and useful discussions.

Author Contributions

Conceptualization: Syed K. Rafi, Irfan Saadi.

Data curation: Syed K. Rafi, Irfan Saadi.

Formal analysis: Syed K. Rafi, Jeremy P. Goering, Adam J. Olm-Shipman, Lauren A. Hipp, Nicholas J. Ernst, Nathan R. Wilson, Everett G. Hall, Sumedha Gunewardena, Irfan Saadi.

Funding acquisition: Irfan Saadi.

Investigation: Syed K. Rafi, Jeremy P. Goering, Adam J. Olm-Shipman, Lauren A. Hipp, Nathan R. Wilson, Everett G. Hall, Sumedha Gunewardena, Irfan Saadi.

Methodology: Syed K. Rafi, Jeremy P. Goering, Adam J. Olm-Shipman, Lauren A. Hipp, Nicholas J. Ernst, Nathan R. Wilson, Everett G. Hall, Sumedha Gunewardena, Irfan Saadi.

Project administration: Irfan Saadi.

Resources: Sumedha Gunewardena, Irfan Saadi.

Software: Adam J. Olm-Shipman, Sumedha Gunewardena.

Supervision: Irfan Saadi.

Validation: Syed K. Rafi, Jeremy P. Goering, Adam J. Olm-Shipman, Lauren A. Hipp, Nicholas J. Ernst, Nathan R. Wilson, Sumedha Gunewardena, Irfan Saadi.

Visualization: Syed K. Rafi, Jeremy P. Goering, Adam J. Olm-Shipman, Lauren A. Hipp, Nicholas J. Ernst, Nathan R. Wilson, Everett G. Hall, Sumedha Gunewardena, Irfan Saadi.

Writing – original draft: Syed K. Rafi, Jeremy P. Goering, Irfan Saadi.

Writing – review & editing: Syed K. Rafi, Jeremy P. Goering, Adam J. Olm-Shipman, Lauren A. Hipp, Nicholas J. Ernst, Nathan R. Wilson, Everett G. Hall, Sumedha Gunewardena, Irfan Saadi.

References

1. McElroy SL, Arnold LM, Shapira NA, Keck PE Jr., Rosenthal NR, Karim MR, et al. Topiramate in the treatment of binge eating disorder associated with obesity: a randomized, placebo-controlled trial. *Am J Psychiatry*. 2003; 160(2):255–61. <https://doi.org/10.1176/appi.ajp.160.2.255> PMID: 12562571
2. Hoopes SP, Reimherr FW, Hedges DW, Rosenthal NR, Kamin M, Karim R, et al. Treatment of bulimia nervosa with topiramate in a randomized, double-blind, placebo-controlled trial, part 1: improvement in binge and purge measures. *J Clin Psychiatry*. 2003; 64(11):1335–41. <https://doi.org/10.4088/jcp.v64n1109> PMID: 14658948
3. Johnson BA, Ait-Daoud N, Bowden CL, DiClemente CC, Roache JD, Lawson K, et al. Oral topiramate for treatment of alcohol dependence: a randomised controlled trial. *Lancet*. 2003; 361(9370):1677–85. [https://doi.org/10.1016/S0140-6736\(03\)13370-3](https://doi.org/10.1016/S0140-6736(03)13370-3) PMID: 12767733
4. Ko YH, Joe SH, Jung IK, Kim SH. Topiramate as an adjuvant treatment with atypical antipsychotics in schizophrenic patients experiencing weight gain. *Clin Neuropharmacol*. 2005; 28(4):169–75. <https://doi.org/10.1097/01.wnf.0000172994.56028.c3> PMID: 16062095

5. Ondo WG, Jankovic J, Connor GS, Pahwa R, Elble R, Stacy MA, et al. Topiramate in essential tremor: a double-blind, placebo-controlled trial. *Neurology*. 2006; 66(5):672–7. <https://doi.org/10.1212/01.wnl.0000200779.03748.0f> PMID: 16436648
6. Koo J, Zavras A. Antiepileptic drugs (AEDs) during pregnancy and risk of congenital jaw and oral malformation. *Oral Dis*. 2013; 19(7):712–20. <https://doi.org/10.1111/odi.12061> PMID: 23305414
7. Meador KJ, Pennell PB, Harden CL, Gordon JC, Tomson T, Kaplan PW, et al. Pregnancy registries in epilepsy: a consensus statement on health outcomes. *Neurology*. 2008; 71(14):1109–17. <https://doi.org/10.1212/01.wnl.0000316199.92256.af> PMID: 18703463
8. MacDonald SC, Bateman BT, McElrath TF, Hernandez-Diaz S. Mortality and Morbidity During Delivery Hospitalization Among Pregnant Women With Epilepsy in the United States. *JAMA Neurol*. 2015; 72(9):981–8. <https://doi.org/10.1001/jamaneurol.2015.1017> PMID: 26147878
9. Hernandez-Diaz S, Huybrechts KF, Desai RJ, Cohen JM, Mogun H, Pennell PB, et al. Topiramate use early in pregnancy and the risk of oral clefts: A pregnancy cohort study. *Neurology*. 2018; 90(4):e342–e51. <https://doi.org/10.1212/WNL.0000000000004857> PMID: 29282333
10. Craig JJ, Hunt SJ. Treating women with juvenile myoclonic epilepsy. *Pract Neurol*. 2009; 9(5):268–77. <https://doi.org/10.1136/jnnp.2009.187898> PMID: 19762886
11. Hunt S, Russell A, Smithson WH, Parsons L, Robertson I, Waddell R, et al. Topiramate in pregnancy: preliminary experience from the UK Epilepsy and Pregnancy Register. *Neurology*. 2008; 71(4):272–6. <https://doi.org/10.1212/01.wnl.0000318293.28278.33> PMID: 18645165
12. Tennis P, Chan KA, Curkendall SM, Li DK, Mines D, Peterson C, et al. Topiramate use during pregnancy and major congenital malformations in multiple populations. *Birth Defects Res A Clin Mol Teratol*. 2015; 103(4):269–75. <https://doi.org/10.1002/bdra.23357> PMID: 25776342
13. Margulis AV, Mitchell AA, Gilboa SM, Werler MM, Mittleman MA, Glynn RJ, et al. Use of topiramate in pregnancy and risk of oral clefts. *Am J Obstet Gynecol*. 2012; 207(5):405 e1–7. <https://doi.org/10.1016/j.ajog.2012.09.001> PMID: 23107084
14. Alsaad AM, Chaudhry SA, Koren G. First trimester exposure to topiramate and the risk of oral clefts in the offspring: A systematic review and meta-analysis. *Reprod Toxicol*. 2015; 53:45–50. <https://doi.org/10.1016/j.reprotox.2015.03.003> PMID: 25797654
15. Holmes LB, Wyszynski DF, Lieberman E. The AED (antiepileptic drug) pregnancy registry: a 6-year experience. *Arch Neurol*. 2004; 61(5):673–8. <https://doi.org/10.1001/archneur.61.5.673> PMID: 15148143
16. Hernandez-Diaz S, Smith CR, Shen A, Mittendorf R, Hauser WA, Yerby M, et al. Comparative safety of antiepileptic drugs during pregnancy. *Neurology*. 2012; 78(21):1692–9. <https://doi.org/10.1212/WNL.0b013e3182574f39> PMID: 22551726
17. Hill DS, Wlodarczyk BJ, Palacios AM, Finnell RH. Teratogenic effects of antiepileptic drugs. *Expert Rev Neurother*. 2010; 10(6):943–59. <https://doi.org/10.1586/ern.10.57> PMID: 20518610
18. Cordero DR, Brugmann S, Chu Y, Bajpai R, Jame M, Helms JA. Cranial neural crest cells on the move: their roles in craniofacial development. *Am J Med Genet A*. 2011; 155A(2):270–9. <https://doi.org/10.1002/ajmg.a.33702> PMID: 21271641
19. Bush JO, Jiang R. Palatogenesis: morphogenetic and molecular mechanisms of secondary palate development. *Development*. 2012; 139(2):231–43. <https://doi.org/10.1242/dev.067082> PMID: 22186724
20. Benjamini Y, Hochberg Y. Controlling the false discovery rate: a practical and powerful approach to multiple testing. *Journal of the Royal Statistical Society Series B (Methodological)*. 1995:289–300.
21. Irizarry RA, Hobbs B, Collin F, Beazer-Barclay YD, Antonellis KJ, Scherf U, et al. Exploration, normalization, and summaries of high density oligonucleotide array probe level data. *Biostatistics*. 2003; 4(2):249–64. <https://doi.org/10.1093/biostatistics/4.2.249> PMID: 12925520
22. Uckun FM, Qazi S, Ma H, Yin L, Cheng J. A rationally designed nanoparticle for RNA interference therapy in B-lineage lymphoid malignancies. *EBioMedicine*. 2014; 1(2–3):141–55. <https://doi.org/10.1016/j.ebiom.2014.10.013> PMID: 25599086
23. He HJ, Zong Y, Bernier M, Wang L. Sensing the insulin signaling pathway with an antibody array. *Proteomics Clin Appl*. 2009; 3(12):1440–50. <https://doi.org/10.1002/prca.200900020> PMID: 21136963
24. Noh MR, Kim SK, Sun W, Park SK, Choi HC, Lim JH, et al. Neuroprotective effect of topiramate on hypoxic ischemic brain injury in neonatal rats. *Exp Neurol*. 2006; 201(2):470–8. <https://doi.org/10.1016/j.expneurol.2006.04.038> PMID: 16884714
25. Sachdeo RC, Sachdeo SK, Walker SA, Kramer LD, Nayak RK, Doose DR. Steady-state pharmacokinetics of topiramate and carbamazepine in patients with epilepsy during monotherapy and concomitant therapy. *Epilepsia*. 1996; 37(8):774–80. <https://doi.org/10.1111/j.1528-1157.1996.tb00651.x> PMID: 8764818

26. May TW, Rambeck B, Jurgens U. Serum concentrations of topiramate in patients with epilepsy: influence of dose, age, and comedication. *Ther Drug Monit.* 2002; 24(3):366–74. <https://doi.org/10.1097/00007691-200206000-00007> PMID: 12021627
27. Berry DJ, Patsalos PN. Comparison of topiramate concentrations in plasma and serum by fluorescence polarization immunoassay. *Ther Drug Monit.* 2000; 22(4):460–4. <https://doi.org/10.1097/00007691-200008000-00016> PMID: 10942188
28. Braga MF, Aroniadou-Anderjaska V, Li H, Rogawski MA. Topiramate reduces excitability in the basolateral amygdala by selectively inhibiting GluK1 (GluR5) kainate receptors on interneurons and positively modulating GABAA receptors on principal neurons. *J Pharmacol Exp Ther.* 2009; 330(2):558–66. <https://doi.org/10.1124/jpet.109.153908> PMID: 19417176
29. Soltani N, Qiu H, Aleksic M, Glinka Y, Zhao F, Liu R, et al. GABA exerts protective and regenerative effects on islet beta cells and reverses diabetes. *Proc Natl Acad Sci U S A.* 2011; 108(28):11692–7. <https://doi.org/10.1073/pnas.1102715108> PMID: 21709230
30. Prud'homme GJ, Glinka Y, Hasilo C, Paraskevas S, Li X, Wang Q. GABA protects human islet cells against the deleterious effects of immunosuppressive drugs and exerts immunoinhibitory effects alone. *Transplantation.* 2013; 96(7):616–23. <https://doi.org/10.1097/TP.0b013e31829c24be> PMID: 23851932
31. Bormann J. Electrophysiological characterization of diazepam binding inhibitor (DBI) on GABAA receptors. *Neuropharmacology.* 1991; 30(12B):1387–9. [https://doi.org/10.1016/s0028-3908\(11\)80006-7](https://doi.org/10.1016/s0028-3908(11)80006-7) PMID: 1723508
32. Akiyama H, Lyons JP, Mori-Akiyama Y, Yang X, Zhang R, Zhang Z, et al. Interactions between Sox9 and beta-catenin control chondrocyte differentiation. *Genes Dev.* 2004; 18(9):1072–87. <https://doi.org/10.1101/gad.1171104> PMID: 15132997
33. Bi W, Huang W, Whitworth DJ, Deng JM, Zhang Z, Behringer RR, et al. Haploinsufficiency of Sox9 results in defective cartilage primordia and premature skeletal mineralization. *Proc Natl Acad Sci U S A.* 2001; 98(12):6698–703. <https://doi.org/10.1073/pnas.111092198> PMID: 11371614
34. Benko S, Fantes JA, Amiel J, Kleinjan DJ, Thomas S, Ramsay J, et al. Highly conserved non-coding elements on either side of SOX9 associated with Pierre Robin sequence. *Nat Genet.* 2009; 41(3):359–64. <https://doi.org/10.1038/ng.329> PMID: 19234473
35. Wagner T, Wirth J, Meyer J, Zabel B, Held M, Zimmer J, et al. Autosomal sex reversal and campomelic dysplasia are caused by mutations in and around the SRY-related gene SOX9. *Cell.* 1994; 79(6):1111–20. [https://doi.org/10.1016/0092-8674\(94\)90041-8](https://doi.org/10.1016/0092-8674(94)90041-8) PMID: 8001137
36. Kwok C, Weller PA, Guioli S, Foster JW, Mansour S, Zuffardi O, et al. Mutations in SOX9, the gene responsible for Campomelic dysplasia and autosomal sex reversal. *Am J Hum Genet.* 1995; 57(5):1028–36. PMID: 7485151
37. Kist R, Schrewe H, Balling R, Scherer G. Conditional inactivation of Sox9: a mouse model for campomelic dysplasia. *Genesis.* 2002; 32(2):121–3. <https://doi.org/10.1002/gene.10050> PMID: 11857796
38. Coricor G, Serra R. TGF-beta regulates phosphorylation and stabilization of Sox9 protein in chondrocytes through p38 and Smad dependent mechanisms. *Sci Rep.* 2016; 6:38616. <https://doi.org/10.1038/srep38616> PMID: 27929080
39. Iordanskaia T, Nawshad A. Mechanisms of transforming growth factor beta induced cell cycle arrest in palate development. *J Cell Physiol.* 2011; 226(5):1415–24. <https://doi.org/10.1002/jcp.22477> PMID: 20945347
40. Iwata J, Parada C, Chai Y. The mechanism of TGF-beta signaling during palate development. *Oral Dis.* 2011; 17(8):733–44. <https://doi.org/10.1111/j.1601-0825.2011.01806.x> PMID: 21395922
41. Gallo EM, Loch DC, Habashi JP, Calderon JF, Chen Y, Bedja D, et al. Angiotensin II-dependent TGF-beta signaling contributes to Loeys-Dietz syndrome vascular pathogenesis. *J Clin Invest.* 2014; 124(1):448–60. <https://doi.org/10.1172/JCI69666> PMID: 24355923
42. Van Laer L, Dietz H, Loeys B. Loeys-Dietz syndrome. *Adv Exp Med Biol.* 2014; 802:95–105. https://doi.org/10.1007/978-94-007-7893-1_7 PMID: 24443023
43. Derynck R, Akhurst RJ, Balmain A. TGF-beta signaling in tumor suppression and cancer progression. *Nat Genet.* 2001; 29(2):117–29. <https://doi.org/10.1038/ng1001-117> PMID: 11586292
44. Bissell DM. Chronic liver injury, TGF-beta, and cancer. *Exp Mol Med.* 2001; 33(4):179–90. <https://doi.org/10.1038/emm.2001.31> PMID: 11795478
45. Schuster N, Krieglstein K. Mechanisms of TGF-beta-mediated apoptosis. *Cell Tissue Res.* 2002; 307(1):1–14. <https://doi.org/10.1007/s00441-001-0479-6> PMID: 11810309
46. Zhu X, Ozturk F, Pandey S, Guda CB, Nawshad A. Implications of TGFbeta on Transcriptome and Cellular Biofunctions of Palatal Mesenchyme. *Front Physiol.* 2012; 3:85. <https://doi.org/10.3389/fphys.2012.00085> PMID: 22514539

47. Ozturk F, Li Y, Zhu X, Guda C, Nawshad A. Systematic analysis of palatal transcriptome to identify cleft palate genes within TGFbeta3-knockout mice alleles: RNA-Seq analysis of TGFbeta3 Mice. *BMC Genomics*. 2013; 14:113. <https://doi.org/10.1186/1471-2164-14-113> PMID: 23421592
48. Li H, Cai H, Deng J, Tu X, Sun Y, Huang Z, et al. TGF-beta-mediated upregulation of Sox9 in fibroblast promotes renal fibrosis. *Biochim Biophys Acta Mol Basis Dis*. 2018; 1864(2):520–32. <https://doi.org/10.1016/j.bbadis.2017.11.011> PMID: 29158184
49. Jara CP, Bobbo VCD, Carraro RS, de Araujo TMF, Lima MHM, Velloso LA, et al. Effects of topical topiramate in wound healing in mice. *Arch Dermatol Res*. 2018; 310(4):363–73. <https://doi.org/10.1007/s00403-018-1822-z> PMID: 29476247
50. Bialer M, White HS. Key factors in the discovery and development of new antiepileptic drugs. *Nat Rev Drug Discov*. 2010; 9(1):68–82. <https://doi.org/10.1038/nrd2997> PMID: 20043029
51. Wee EL, Norman EJ, Zimmerman EF. Presence of gamma-aminobutyric acid in embryonic palates of AJ and SWV mouse strains. *J Craniofac Genet Dev Biol*. 1986; 6(1):53–61. PMID: 3700592
52. Hagiwara N, Katarova Z, Siracusa LD, Brilliant MH. Nonneuronal expression of the GABA(A) beta3 subunit gene is required for normal palate development in mice. *Dev Biol*. 2003; 254(1):93–101. [https://doi.org/10.1016/s0012-1606\(02\)00030-1](https://doi.org/10.1016/s0012-1606(02)00030-1) PMID: 12606284
53. Asada H, Kawamura Y, Maruyama K, Kume H, Ding RG, Kanbara N, et al. Cleft palate and decreased brain gamma-aminobutyric acid in mice lacking the 67-kDa isoform of glutamic acid decarboxylase. *Proc Natl Acad Sci U S A*. 1997; 94(12):6496–9. <https://doi.org/10.1073/pnas.94.12.6496> PMID: 9177246
54. Andang M, Hjerling-Leffler J, Moliner A, Lundgren TK, Castelo-Branco G, Nanou E, et al. Histone H2AX-dependent GABA(A) receptor regulation of stem cell proliferation. *Nature*. 2008; 451(7177):460–4. <https://doi.org/10.1038/nature06488> PMID: 18185516
55. White HS, Brown SD, Woodhead JH, Skeen GA, Wolf HH. Topiramate enhances GABA-mediated chloride flux and GABA-evoked chloride currents in murine brain neurons and increases seizure threshold. *Epilepsy Res*. 1997; 28(3):167–79. [https://doi.org/10.1016/s0920-1211\(97\)00045-4](https://doi.org/10.1016/s0920-1211(97)00045-4) PMID: 9332882
56. Asbun J, Villarreal FJ. The pathogenesis of myocardial fibrosis in the setting of diabetic cardiomyopathy. *J Am Coll Cardiol*. 2006; 47(4):693–700. <https://doi.org/10.1016/j.jacc.2005.09.050> PMID: 16487830
57. Hassan JH, Chelucci C, Peschle C, Sorrentino V. Transforming growth factor beta (TGF-beta) inhibits expression of fibrinogen and factor VII in a hepatoma cell line. *Thromb Haemost*. 1992; 67(4):478–83. PMID: 1321511
58. Chetaille P, Preuss C, Burkhard S, Cote JM, Houde C, Castilloux J, et al. Mutations in SGOL1 cause a novel cohesinopathy affecting heart and gut rhythm. *Nat Genet*. 2014; 46(11):1245–9. <https://doi.org/10.1038/ng.3113> PMID: 25282101
59. Aggarwal K, Massague J. Ubiquitin removal in the TGF-beta pathway. *Nat Cell Biol*. 2012; 14(7):656–7. <https://doi.org/10.1038/ncb2534> PMID: 22743709
60. Eickelberg O, Kohler E, Reichenberger F, Bertschin S, Woodtli T, Erne P, et al. Extracellular matrix deposition by primary human lung fibroblasts in response to TGF-beta1 and TGF-beta3. *Am J Physiol*. 1999; 276(5 Pt 1):L814–24. <https://doi.org/10.1152/ajplung.1999.276.5.L814> PMID: 10330038
61. McKean DM, Niswander L. Defects in GPI biosynthesis perturb Cripto signaling during forebrain development in two new mouse models of holoprosencephaly. *Biol Open*. 2012; 1(9):874–83. <https://doi.org/10.1242/bio.20121982> PMID: 23213481
62. Chung Y, Fu E. Crosstalk between Shh and TGF-beta signaling in cyclosporine-enhanced cell proliferation in human gingival fibroblasts. *PLoS One*. 2013; 8(7):e70128. <https://doi.org/10.1371/journal.pone.0070128> PMID: 23922933